Negative charge and charging dynamics in Al2O3 films on Si characterized by second-harmonic generation

Negative charge and charging dynamics in Al_2O_3 films on Si characterized by second-harmonic generation

J. J. H. Gielis,[a] B. Hoex, M. C. M. van de Sanden, and W. M. M. Kessels
Department of Applied Physics, Eindhoven University of Technology, P.O. Box 513, 5600 MB Eindhoven, The Netherlands

(Received 13 May 2008; accepted 29 July 2008; published online 1 October 2008)

Thin films of Al_2O_3 synthesized by atomic layer deposition provide an excellent level of interface passivation of crystalline silicon (*c*-Si) after a postdeposition anneal. The Al_2O_3 passivation mechanism has been elucidated by contactless characterization of *c*-Si/Al_2O_3 interfaces by optical second-harmonic generation (SHG). SHG has revealed a *negative* fixed charge density in as-deposited Al_2O_3 on the order of 10^{11} cm^{-2} that increased to $10^{12}-10^{13}$ cm^{-2} upon anneal, causing effective field-effect passivation. In addition, multiple photon induced charge trapping dynamics suggest a reduction in recombination channels after anneal and indicate a *c*-Si/Al_2O_3 conduction band offset of 2.02 ± 0.04 eV. © *2008 American Institute of Physics*.
[DOI: 10.1063/1.2985906]

I. INTRODUCTION

The reduction in recombination losses at semiconductor interfaces is of prime importance for numerous photonic devices such as nanocrystal or wafer-based light emitting diodes, photodetectors, and high-efficiency solar cells. Recombination of charge carriers at an interface can be suppressed by passivating the interface. Recently, interface passivation by Al_2O_3 films has been reported for III-V compound semiconductors[1] and for crystalline Si (*c*-Si).[2–5] Thin passivation layers of Al_2O_3 synthesized by atomic layer deposition (ALD) were demonstrated to enhance the efficiency of light emission from *c*-Si, even outperforming thermal SiO_2,[3] while Al_2O_3 films deposited by plasma-assisted ALD followed by a postdeposition anneal were shown to provide excellent interface passivation of both *n*-type and *p*-type *c*-Si.[4,5] In general, interface passivation can be achieved by a reduction in recombination centers, typically interface defects, or by electrostatic shielding of charge carriers by internal electric fields. The passivation properties of Al_2O_3 films are likely related to *negative* fixed charge in Al_2O_3, providing field-effect passivation.[6] Real-time characterization of the fixed charge density in the Al_2O_3 films and the Al_2O_3 interface properties during processing could help to unravel the exact passivation mechanism.

In this respect, the noninvasive nonlinear optical technique of second-harmonic generation (SHG) is a very promising diagnostic. SHG is highly interface sensitive for centrosymmetric media and allows for a contactless detection of internal electric fields, which can either be applied static fields or electric fields in semiconductor space-charge regions arising from interfacial charge separation.[7,8] The effect of electric field-induced SHG (EFISH) has been used to study charge trapping in the *c*-Si/SiO_2 system.[9–12] More recently, photon induced charge trapping,[13,14] as well as process-dependent charging in high-*k* dielectric stacks have been investigated.[15,16]

In this paper we characterize as-grown and annealed Si(100)/Al_2O_3 structures with interfacial SiO_x synthesized by plasma-assisted ALD using both spectroscopic and time-dependent SHG. With spectroscopic SHG, the polarity of the fixed charge in the Al_2O_3 is determined to be negative and the fixed charge density is deduced, exhibiting a strong increase after anneal. In addition, with time-dependent SHG, an improvement in interface properties is observed after anneal and the *c*-Si/Al_2O_3 conduction band offset is derived. These results provide important insight into the interface passivation properties of Al_2O_3, and directly illustrate the feasibility of SHG as a contactless technique to characterize charge and charging dynamics in *c*-Si/high-*k* dielectric structures *in situ* and during processing.

II. EXPERIMENT

Amorphous Al_2O_3 films were deposited at both sides of 275 μm thick P-doped H terminated Si(100) wafers with a resistivity of 1.9 Ω cm by plasma-assisted ALD using alternating $Al(CH_3)_3$ dosing and O_2 plasma exposure at a substrate temperature of 200 °C. After being analyzed, the as-grown samples were annealed for 30 min at 425 °C in N_2. More details on the preparation of the Al_2O_3 films and their analysis, demonstrating for example a stoichiometric composition ([O]/[Al]=1.5), can be found in Ref. 17. High resolution transmission electron microscopy (HRTEM) revealed the presence of an interfacial SiO_x layer of ~1.5 nm between the Si(100) and the Al_2O_3 both before and after anneal, with the Al_2O_3 remaining amorphous after anneal.[4] With carrier lifetime spectroscopy the effective lifetimes of *c*-Si passivated by as-grown Al_2O_3 were determined to be <10 μs, which are indistinguishable from an unpassivated *c*-Si wafer, whereas, after anneal, lifetimes up to 6.6 ms were obtained, corresponding to an excellent level of surface passivation.[4,5] The SHG experiments were carried out at an angle of incidence of 35° using a Ti:sapphire oscillator providing radiation tunable in the 1.33–1.75 eV photon energy

[a]Electronic mail: j.j.h.gielis@tue.nl

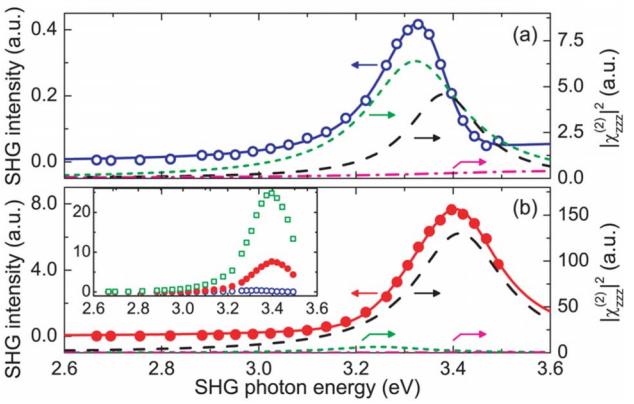

FIG. 1. (Color online) SHG spectra for an 11 nm Al_2O_3 film on Si(100), (a) as deposited (sample A1) and (b) after anneal (sample A2). The solid lines are fits to the data using a superposition of three CP-like resonances. The dashed lines represent the individual resonances. Data were obtained at *p* polarized fundamental and SHG radiation using a laser power at the sample of 40 mW (fluence 25 μJ cm^{-2} per pulse). In the inset in (b) the SHG spectra for sample A1 (open circles), sample A2 (closed circles), and an annealed 26 nm thick Al_2O_3 film on Si(100) (open squares, sample B) are shown on the same scale.

range with a pulse duration of ~90 fs.[18] Time-dependent SHG experiments were performed at a time resolution of 0.1 s.

III. RESULTS AND DISCUSSION

In Figs. 1(a) and 1(b) SHG spectra for *p*-polarized fundamental and SHG radiation are shown for a 11 nm thick Al_2O_3 film on Si(100), as grown (sample A1) and after anneal (sample A2), respectively. For comparison the spectra are combined in the inset. Both show a distinct resonance in the 3.3–3.4 eV range, indicating that the SHG response is dominated by *c*-Si interband transitions at the E_0'/E_1 critical point (CP).[19,20] The anneal very clearly modifies the SHG spectrum; the amplitude increases with more than an order of magnitude, whereas the peak shifts from ~3.3 to ~3.4 eV resulting in a more symmetric feature.

In order to separate different contributions to the SHG response, the spectra have been reproduced using a model in which the SHG intensity is approximated by a coherent superposition of CP-like resonances with excitonic line shapes evaluated at the substrate/film interface[18,21,22]

$$I(2\omega) = \left| A_{zzz}(\omega,\theta) \sum_q \chi^{(2)}_{zzz,q} \right|^2 I^2_{\mathrm{in}}(\omega) \propto \left| A_{zzz}(\omega,\theta) \sum_q \frac{h_q e^{i\varphi_q}}{2\omega - \omega_q + i\Gamma_q} \right|^2 I^2_{\mathrm{in}}(\omega), \quad (1)$$

where h_q denotes the (real) amplitude, ω_q the frequency, Γ_q the linewidth, and φ_q the excitonic phase of resonance q. The spectra have been analyzed in terms of tensor element $\chi^{(2)}_{zzz}$, as including the other elements contributing to *p*-polarized fundamental and SHG radiation, $\chi^{(2)}_{zxx}$ and $\chi^{(2)}_{xxz}$,[7] does not modify the spectral parameters significantly. The complex function $A_{zzz}(\omega,\theta)$ in Eq. (1) describes the propagation of the fundamental and SHG radiation in the film-substrate system. This film thickness dependent function includes linear optical effects, such as absorption, refraction, and interference due to multiple reflections within the Al_2O_3 films.[18]

The spectrum for the as-grown Al_2O_3 film (A1) clearly has an asymmetric shape, indicating the presence of multiple interfering contributions. The data can be fitted very well when taking into account three contributions with their parameters listed in Table I. The individual resonances, shown in Fig. 1(a), consist of a main contribution at 3.32 ± 0.01 eV, and additional contributions at 3.38 ± 0.01 and 3.62 eV. The resonance frequency and linewidth of the third contribution are fixed at 3.62 and 0.36 eV, as within the current experimental photon energy range, the parameters of this contribution cannot be determined unambiguously. These latter values have been reported by Rumpel *et al.* for *c*-Si/SiO_2, and have been attributed to a resonance related to Si interband transitions in a thin transition layer between Si and SiO_2.[23,24] The presence of such an interface resonance seems also viable for the Si/Al_2O_3 system, especially considering the presence of the interfacial SiO_x layer as detected by HRTEM. Also, the parameters of the resonances at 3.32 ± 0.01 and 3.38 ± 0.01 eV correspond well to values reported for the *c*-Si/SiO_2 interface,[24] as well as to values reported for clean and H dosed *c*-Si surfaces.[20] In addition to the good reproduction of the experimental data, this similarity supports the validity of the fitting results.

Moreover, the SHG spectrum after anneal (sample A2) can also be reproduced very well by the same resonances, as shown in Table I and Fig. 1(b). The second contribution at 3.414 ± 0.004 eV is clearly dominant with an amplitude that increased by a factor of six compared to sample A1. The first contribution has redshifted to 3.25 ± 0.02 eV and has minor impact. This contribution can be assigned to interband transitions related to Si-Si bonds modified due to the vicinity of the interface with the film.[19,20] The redshift of this "modified Si-Si interface contribution" after anneal might be related to further weakening of Si-Si bonds,[19,23] indicating structural changes in the (interfacial) oxide.

The resonance around 3.40 eV is a clear signature of EFISH originating from the bulk space-charge region (SCR) in the *c*-Si.[20] The Si SCR is predominantly caused by fixed charge in the Al_2O_3, as illustrated in Fig. 2(b). The drastic

TABLE I. Parameters of the three CP resonances as obtained from the fits to the SHG spectra for Al_2O_3 on Si(100): 11 nm Al_2O_3 as-grown (A1) and after anneal (A2), and 26 nm Al_2O_3 after anneal (B). In the analysis φ_1 is set to 0. Parameter values in italic were fixed in the analysis.

	Modified Si-Si interface contribution			EFISH contribution				Oxide related interface contribution			
	h_1 (arb. units)	$\hbar\omega_1$ (eV)	$\hbar\Gamma_1$ (eV)	h_2 (arb. units)	$\hbar\omega_2$ (eV)	$\hbar\Gamma_2$ (eV)	φ_2 (π rad)	h_3 (arb. units)	$\hbar\omega_3$ (eV)	$\hbar\Gamma_3$ (eV)	φ_3 (π rad)
A1	0.31 ± 0.05	3.32 ± 0.01	0.121 ± 0.009	0.19 ± 0.07	3.38 ± 0.01	0.09 ± 0.01	0.9 ± 0.1	0.23 ± 0.12	*3.62*	*0.36*	0.33 ± 0.07
A2	*0.31*	3.25 ± 0.02	*0.121*	1.21 ± 0.05	3.414 ± 0.004	0.114 ± 0.004	1.00 ± 0.06	*0.23*	*3.62*	*0.36*	*0.33*
B	*0.31*	3.23 ± 0.02	*0.121*	2.11 ± 0.09	3.396 ± 0.004	0.117 ± 0.003	1.0 ± 0.1	*0.23*	*3.62*	*0.36*	*0.33*

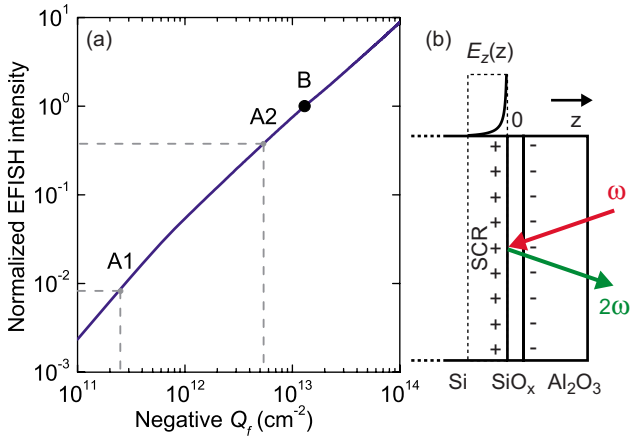

FIG. 2. (Color online) (a) EFISH intensity at a SHG photon energy of 3.40 eV as a function of negative fixed charge density Q_f in Al_2O_3. The relation is calibrated and normalized using the CP parameters for an annealed 26 nm Al_2O_3 film on Si(100) (sample B) with a known Q_f. A1 and A2 indicate the charge and EFISH intensities for an 11 nm Al_2O_3 film on Si(100) before and after anneal, respectively. (b) Schematic of the Si(100)/Al_2O_3 interface with Si SCR and interfacial SiO_x.

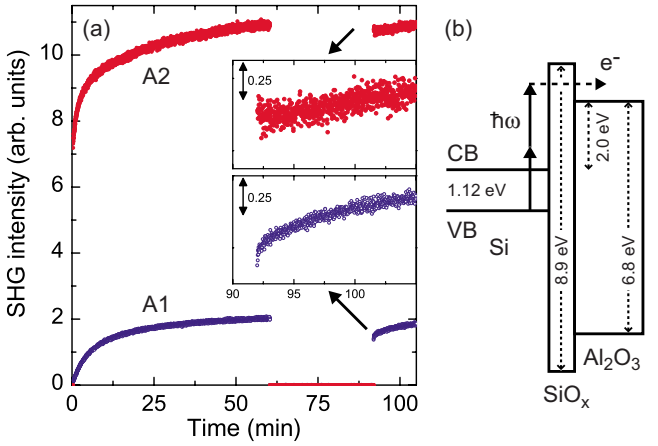

FIG. 3. (Color online) (a) Time-dependent SHG intensity for 11 nm Al_2O_3 on Si(100) before (open circles, A1) and after anneal (closed circles, A2) for a fundamental photon energy of 1.71 eV, and an average laser power of 100 mW. Between $t=60-92$ min the laser beam was blocked. The insets show the SHG intensity during the second period of illumination in greater detail. (b) Energy diagram illustrating photon induced charge injection.

increase in the EFISH contribution after anneal is a clear indication for the increase in the fixed charge density Q_f in the Al_2O_3. The electric field at the interface with Al_2O_3, resulting from the doping of the *c*-Si substrates (2.5×10^{15} cm^{-3}), can be estimated to be <10 kV cm^{-1},[25,26] which is too low to have a significant effect on the SHG response.[8,20] As shown in Table I, the phase difference between the contribution due to the Si-Si interface bonds and the EFISH contribution is $\sim\pi$ both before and after anneal, which indicates a *positively* charged Si SCR,[24] and thus *negative* fixed charge in the Al_2O_3. Electrical characterization of Al_2O_3 films has revealed the presence of negative fixed charge situated predominantly at the interface with interfacial SiO_x.[27]

The intensity of the EFISH contribution resulting from the CP modeling reflects the magnitude of the electric field $E_z^{DC}(z)$ in the Si SCR and can be used to quantify the negative Q_f in the Al_2O_3 before and after anneal. To achieve this, the negative Q_f can be related to the electric field $E_z^{DC}(z)$ in the Si SCR by numerically integrating Poisson's equation. Subsequent integration of $E_z^{DC}(z)$ over the SCR, taking into account the penetration and escape depths of the fundamental and SHG radiation, gives the EFISH electric field and, hence, the EFISH intensity:[8,20]

$$I^{\mathrm{EFISH}}(2\omega) \sim \left| \vec{\chi}^{(3)}:\mathbf{E}(\omega)\mathbf{E}(\omega)\int_{-\infty}^{0} \mathrm{e}^{-i(K_z+2k_z)z}E_z^{DC}(z)dz \right|^2, \tag{2}$$

where K_z and k_z are the complex wave vector components of the SHG and fundamental radiation perpendicular to the *c*-Si/Al_2O_3 interface, respectively. To relate the EFISH intensity to absolute values of Q_f in the Al_2O_3, a 26 nm thick annealed Al_2O_3 film on Si(100) (sample B) with a known negative Q_f of $(1.3\pm0.1)\times10^{13}$ cm^{-2}, as measured in a corona charging experiment, was used for calibration.[6] This value of Q_f yields an electric field at the position of the interface of $E_z^{DC}(0)=2.1$ MV cm^{-1}, corresponding to a strong EFISH contribution. The SHG spectrum of this film is shown in the inset of Fig. 1 and the parameters obtained from CP modeling are included in Table I. In Fig. 2(a) the EFISH intensity calculated using Eq. (2) is shown as a function of the negative Q_f in the Al_2O_3. As indicated in Fig. 2(a), the EFISH intensity deduced from the CP modeling can be related to a negative fixed charge density of $Q_f=2.5\times10^{11}$ cm^{-2} for the as-grown 11 nm thick Al_2O_3 film (A1), whereas after anneal (A2) Q_f has increased to 5.4×10^{12} cm^{-2} for this sample. These values, which are in good agreement with results obtained by conventional capacitance-voltage analysis,[6] indicate that the field-effect passivation improves significantly upon anneal.

The SHG spectra were obtained using a laser power at the sample of 40 mW (fluence 25 μJ cm^{-2} per pulse) while keeping the illumination time as short as possible, since at higher laser power the SHG intensity increases strongly with illumination time due to photon induced charge injection into the Al_2O_3. In Fig. 3(a) the charging dynamics are shown before and after anneal of sample A, using a laser power of 100 mW and a fundamental photon energy of 1.71 eV. The initial SHG intensity (at $t=0$ min) is higher after anneal, in agreement with the spectroscopic data. The rapid increase in SHG intensity during illumination reflects an increase in the EFISH contribution caused by the charge injection. Both for SiO_2 and high-*k* dielectrics on *c*-Si, the charge transfer process has been reported to occur via injection of electrons from the *c*-Si valence band into the oxide conduction band, as illustrated in Fig. 3(b). The injected charge then diffuses into trap sites in either the oxide bulk at the buried interface or at the ambient surface.[10,14,16,28] The monotonous increase in the SHG intensity in Fig. 3(a) indicates that the laser induced trapped charge in the oxide has the same polarity as the fixed charge, i.e., negative, hence hole injection is expected to be insignificant. The data also show that after anneal more charge can be injected. The total negative charge after 60 min of illumination at the conditions in Fig. 3(a) can be estimated to be 2.0×10^{12} and 8.7×10^{12} cm^{-2} for the

as-grown and annealed samples, respectively. This estimate is based on the assumptions that the negative charge is situated at the interface and that only the amplitude h_2 of the EFISH contribution increases, whereas all other contributions and parameters remain unaltered by the photon induced charge injection.

After 60 min of illumination the laser beam is blocked for 32 min. The behavior during the second period of illumination is clearly different before and after anneal. The laser induced SHG intensity for the as-grown film has decreased with 30% and rapidly increases again, similar to the initial illumination. The annealed film displays a decrease of only 4% and exhibits a slowly increasing trend similar as just before blocking of the laser beam. The total charge density right after unblocking the laser beam can be estimated to be 1.6×10^{12} and 8.6×10^{12} cm^{-2} for the as-grown and annealed film, respectively. The limited decrease in charge density for the annealed sample indicates that the detrapping of laser induced trapped charge has been reduced after anneal compared to the as-deposited state. This effect suggests a reduction in detrapping channels in the Al_2O_3, in the interfacial SiO_x, or at the different interfaces. Detrapping might occur by tunneling of electrons through the interfacial oxide followed by recombination with holes at the interface. An improvement of the interfacial SiO_x properties after anneal, as also observed with Fourier transform infrared spectroscopy,[29] might reduce the tunneling of the photon induced trapped charge back into the Si. The reduction in detrapping channels might also account for the excellent level of surface passivation observed for Al_2O_3 films after anneal, in addition to the increase in the internal electric field.[4,29]

The time evolution of the SHG intensity can provide more information on the electronic properties of the c-Si/Al_2O_3 system. To model the time dependence, a simple first-order rate equation is used to describe the photon induced charge injection kinetics,[9,12]

$$\frac{dn_i}{dt} = (n_{0i} - n_i)/\tau_{ti} - n_i/\tau_{di}, \tag{3}$$

where n_i denotes the density of filled charge traps of type i, n_{0i} the initial density of unfilled traps, τ_{ti}^{-1} the trapping rate, and τ_{di}^{-1} the detrapping rate. If the traps are initially empty then the solution to Eq. (3) is given by

$$n_i(t) = \frac{n_{0i}\tau_{di}}{\tau_{ti} + \tau_{di}}(1 - e^{-(\tau_{ti}^{-1}+\tau_{di}^{-1})t}). \tag{4}$$

Following this model with multiple traps, the time dependence of the laser induced SHG intensity can be written as

$$I(2\omega,t) = \left| a_0 + \sum_{i=1}^{m} a_i(1 - e^{-t/\tau_i}) \right|^2, \tag{5}$$

where $\tau_i^{-1} = (\tau_{ti}^{-1} + \tau_{di}^{-1})$, and where a_0 and a_i are constants related to the initial and saturation SHG intensities, and the relative contribution of each type of trap i. Equation (5) can be fitted best to the data when using a description with three types of charge traps ($m=3$). The existence of multiple types of traps has been reported for the extensively studied c-Si/SiO_2 system both in the SiO_2 bulk, and at surfaces and interfaces.[10,30] For the conditions shown in Fig. 3(a) the fitting procedure results in $\tau_1=89$ s, $\tau_2=351$ s, and $\tau_3=1801$ s before anneal, and $\tau_1=38$ s, $\tau_2=154$ s, and $\tau_3=1704$ s after anneal, where all time constants have an uncertainty of 5%. Consequently, the annealing not only increases Q_f, it also increases the net rate at which charge can be injected into the oxide.

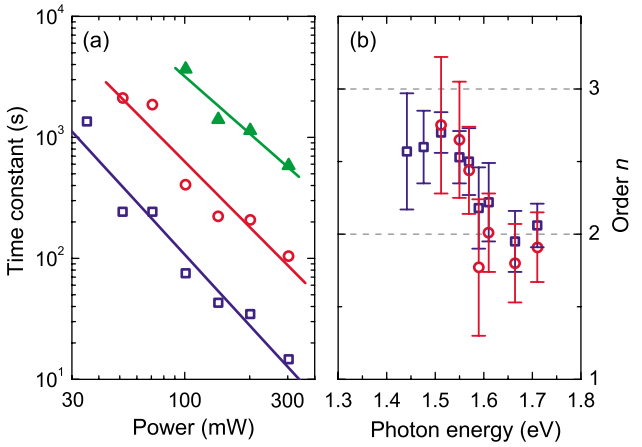

FIG. 4. (Color online) (a) Laser power dependence of the three time constants for 11 nm Al_2O_3 after anneal (sample A2) at a fundamental photon energy of 1.66 eV. The solid lines are fits to the data. (b) Order of the electron injection process as a function of fundamental photon energy.

The time constants strongly depend on the laser power applied, indicating that the photon induced charge trapping is a process involving multiple photons. In Fig. 4(a) this dependence is shown for sample A2 at a fundamental photon energy of 1.66 eV. For lower laser powers, the slowest time constants are omitted in the analysis as they exceed the measurement time and have a minor contribution to the observed time-dependent behavior. Figure 3(a) shows that the detrapping rates τ_{di}^{-1} for the annealed sample are much slower than the trapping rates τ_{ti}^{-1}, hence $\tau_i^{-1} \approx \tau_{ti}^{-1}$. The number of photons n required to inject the charge from the c-Si into the oxide can be deduced by fitting the intensity dependence of the time constants to $\tau_i^{-1} \propto [I_{in}(\omega)]^n$.[9,12] The result of this analysis performed for different photon energies is shown in Fig. 4(b) for the two fastest time constants. In the fundamental photon energy range of 1.59–1.55 eV, a transition in the number of photons required to inject charge from the c-Si into the oxide from $n=2$ to $n=3$ can be observed. This transition reflects the threshold for two-photon electron injection from the c-Si valence band into the oxide conduction band.[12] Taking into account the c-Si band gap of 1.12 eV, this yields a c-Si/oxide conduction band offset of 2.02 ± 0.04 eV. This value indicates that the c-Si/oxide conduction band offset is not governed by the interfacial SiO_x of ~1.5 nm, considering the higher c-Si/SiO_2 conduction band offset of 3.1 eV.[26] These results are consistent with values for the conduction band offset for the c-Si/Al_2O_3 system obtained by Afanas'ev *et al.* using internal photoemission experiments, including their observation that a 1.2 nm thick interfacial thermal SiO_2 layer between c-Si and Al_2O_3 hardly changes the c-Si/Al_2O_3 conduction band offset.[31] The conduction band offset of ~2.0 eV indicates also that the influence of hole injection from the c-Si conduction band into the oxide valence band is

limited. Considering the band gap of Al_2O_3 deposited with ALD of 6.8 eV,[32] the c-Si/Al_2O_3 valence band offset is ~3.7 eV, hence the hole injection process would require at least one photon more than the electron injection process.

IV. CONCLUSIONS

Al_2O_3 thin films deposited on Si(100) by plasma-assisted ALD have been studied by spectroscopic and time-dependent SHG before and after annealing. The Al_2O_3 films contain fixed charge, which is *negative*, with a density increasing from $\sim 10^{11}$ cm^{-2} before anneal to $10^{12}-10^{13}$ cm^{-2} after anneal. Furthermore, due to the annealing, both the amount of charge that can be injected into the Al_2O_3 and the net rate at which this charge can be injected increased, whereas detrapping channels in the c-Si/Al_2O_3 system are reduced. The excellent passivation properties of Al_2O_3 after annealing are likely a result of the increase in the internal electric field with an additional reduction in interface defects.[29] The results demonstrate the feasibility of SHG for contactless characterization of charge and charging dynamics in c-Si/high-k dielectric structures *in situ* and during processing. This kind of analysis is inaccessible by conventional techniques such as capacitance-voltage measurements; moreover, SHG studies do not require a minimum film thickness. The application of SHG during processing of c-Si/high-k structures provides not only relevant information for devices relying on field-effect passivation but also for nonvolatile memory and metal-oxide-semiconductor transistor applications.

ACKNOWLEDGMENTS

The authors thank W. Keuning for the Al_2O_3 depositions, and M.J.F. van de Sande, J.F.C. Jansen, J.J.A Zeebregts, and R.F. Rumphorst for their skillful technical assistance. This work was supported by the Netherlands Foundation for Fundamental Research on Matter (FOM).

[1] M. L. Huang, Y. C. Chang, C. H. Chang, Y. J. Lee, P. Chang, J. Kwo, T. B. Wu, and M. Hong, Appl. Phys. Lett. **87**, 252104 (2005).
[2] G. Agostinelli, A. Delabie, P. Vitanov, Z. Alexieva, H. F. W. Dekkers, S. de Wolf, and G. Beaucarne, Sol. Energy Mater. Sol. Cells **90**, 3438 (2006).
[3] M. J. Chen, Y. T. Shih, M. K. Wu, and F. Y. Tsai, J. Appl. Phys. **101**, 033130 (2007).
[4] B. Hoex, S. B. S. Heil, E. Langereis, M. C. M. van de Sanden, and W. M. M. Kessels, Appl. Phys. Lett. **89**, 042112 (2006).
[5] B. Hoex, J. Schmidt, R. Bock, P. P. Altermatt, M. C. M. van de Sanden, and W. M. M. Kessels, Appl. Phys. Lett. **91**, 112107 (2007).
[6] B. Hoex, J. Schmidt, P. Pohl, M. C. M. van de Sanden, and W. M. M. Kessels, J. Appl. Phys. **104**, 044903 (2008).
[7] T. F. Heinz, in *Nonlinear Surface Electromagnetic Phenomena*, edited by H. E. Ponath and G. I. Stegeman (Elsevier, Amsterdam, 1991).
[8] O. A. Aktsipetrov, A. A. Fedyanin, E. D. Mishina, A. N. Rubtsov, C. W. van Hasselt, M. A. C. Devillers, and Th. Rasing, Phys. Rev. B **54**, 1825 (1996).
[9] J. G. Mihaychuk, J. Bloch, Y. Liu, and H. M. van Driel, Opt. Lett. **20**, 2063 (1995).
[10] J. Bloch, J. G. Mihaychuk, and H. M. van Driel, Phys. Rev. Lett. **77**, 920 (1996).
[11] G. Lüpke, Surf. Sci. Rep. **35**, 75 (1999).
[12] Z. Marka, R. Pasternak, S. N. Rashkeev, Y. Jiang, S. T. Pantelides, N. H. Tolk, P. K. Roy, and J. Kozub, Phys. Rev. B **67**, 045302 (2003).
[13] Y. D. Glinka, W. Wang, S. K. Singh, Z. Marka, S. N. Rashkeev, Y. Shirokaya, R. Albridge, S. T. Pantelides, N. H. Tolk, and G. Lucovsky, Phys. Rev. B **65**, 193103 (2002).
[14] V. Fomenko, E. P. Gusev, and E. Borguet, J. Appl. Phys. **97**, 083711 (2005).
[15] R. Carriles, J. Kwon, Y. Q. An, M. C. Downer, J. Price, and A. C. Diebold, Appl. Phys. Lett. **88**, 161120 (2006).
[16] R. Carriles, J. Kwon, Y. Q. An, L. Sun, S. K. Stanley, J. G. Ekerdt, M. C. Downer, J. Price, T. Boeskce, and A. C. Diebold, J. Vac. Sci. Technol. B **24**, 2160 (2006).
[17] J. L. van Hemmen, S. B. S. Heil, J. H. Klootwijk, F. Roozeboom, C. J. Hodson, M. C. M. van de Sanden, and W. M. M. Kessels, J. Electrochem. Soc. **154**, G165 (2007).
[18] J. J. H. Gielis, P. M. Gevers, A. A. E. Stevens, H. C. W. Beijerinck, M. C. M. van de Sanden, and W. M. M. Kessels, Phys. Rev. B **74**, 165311 (2006).
[19] W. Daum, H.-J. Krause, U. Reichel, and H. Ibach, Phys. Rev. Lett. **71**, 1234 (1993).
[20] J. I. Dadap, Z. Xu, X. F. Hu, M. C. Downer, N. M. Russell, J. G. Ekerdt, and O. A. Aktsipetrov, Phys. Rev. B **56**, 13367 (1997).
[21] G. Erley, R. Butz, and W. Daum, Phys. Rev. B **59**, 2915 (1999).
[22] P. Lautenschlager, M. Garriga, L. Viña, and M. Cardona, Phys. Rev. B **36**, 4821 (1987).
[23] G. Erley and W. Daum, Phys. Rev. B **58**, R1734 (1998).
[24] A. Rumpel, B. Manschwetus, G. Lilienkamp, H. Schmidt, and W. Daum, Phys. Rev. B **74**, 081303 (2006).
[25] W. Mönch, P. Koke, and S. Krueger, J. Vac. Sci. Technol. **19**, 313 (1981).
[26] S. M. Sze, *Physics of SemiConductor Devices* (Wiley, New York, 1981).
[27] J. A. Aboaf, D. R. Kerr, and E. Bassous, J. Electrochem. Soc. **120**, 1103 (1973).
[28] The role of surface contaminants in the charge trapping process is minor; SHG experiments during and after degassing of sample A2 in vacuum resulted in the same response as observed in ambient air.
[29] B. Hoex, J. J. H. Gielis, M. C. M. van de Sanden, and W. M. M. Kessels, J. Appl. Phys. (unpublished).
[30] C. Svensson, in *The* Si-SiO_2 *System*, edited by P. Balk (Elsevier, Amsterdam, 1988).
[31] V. V. Afanas'ev, M. Houssa, A. Stesmans, and M. M. Heyns, Appl. Phys. Lett. **78**, 3073 (2001).
[32] J. Robertson, Solid-State Electron. **49**, 283 (2005).